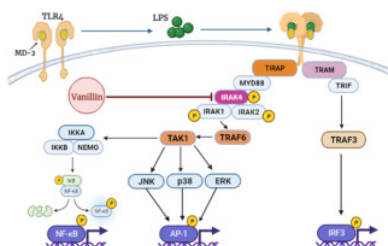


Sl. No.	<p style="text-align: center;">IIT Ropar List of Recent Publications with Abstract Coverage: February, 2023</p>
1.	<p>6-bit 1-gs/s partially active flash adc with comparator offset correction N Sharma, V Hande, RK Srivastava, DM Das - IEEE International Symposium on Smart Electronic Systems, 2022</p> <p>Abstract: This paper presents a low-power 6-bit 1 GS/s partially active flash analog-to-digital converters (ADC) in 65-nm CMOS technology. A novel comparator offset correction technique is proposed, which does not require additional foreground calibration cycles. The partially active second-stage comparison is employed for power efficiency. A third-stage comparison is introduced for offset correction using fifteen low-offset comparators, out of which two are activated. The 0.5-bit redundancy from the first-stage provides the tolerance to track-and-hold (T/H) buffer settling error for high-speed applications. The simulation results show that the ADC achieves a signal-to-noise and distortion ratio (SNDR) of 36.36 dB and a spurious-free dynamic range (SFDR) of 48.65 dB at a Nyquist frequency of 500 MHz with the power consumption of 13.98 mW.</p>
2.	<p>A case study on periodic spatio- temporal hotspot detection in azure traffic data VMV Gunturi, R Rajeev, V Bondre, A Barnwal, S Jain... - IEEE International Conference on Data Mining Workshops, 2022</p> <p>Abstract: Given a spatio-temporal event framework E and a collection of time-stamped events A (over E), the goal of the periodic spatio-temporal hotspot detection (PST-Hotspot) problem is to determine spatial regions which show high “intensity” of events at certain periodic intervals. The output of the PST-Hotspot detection problem consists of the following: (a) a collection of spatial regions (which show high intensity of events) and, (b) their respective time intervals of high activity and periodicity values (e.g., daily, weekday-only, etc). PST-Hotspot detection poses significant challenge for designing a suitable interest measure. The aim over here is to design a mathematical representation of a PST-Hotspot such that it can differentiate interesting periodic patterns from trivial persistent patterns in the dataset. The current state of the art in the area of spatial and spatio-temporal hotspot detection focus on non-periodic patterns. In contrast, our proposed approach is able to determine periodic hotspots. We experimentally evaluated our proposed algorithm using real Azure traffic dataset from the Indian region.</p>
3.	<p>A holographic study of the characteristics of chaos and correlation in the presence of backreaction S Chakraborty, S Hoshino, S Pant, K Sil - Physics Letters B, 2023</p> <p>Abstract: In this work, we perform a holographic study to estimate the effect of backreaction on the correlation between two subsystems forming the thermofield double (TFD) state. Each of these subsystems is described as a strongly coupled large-N_C thermal field theory, and the backreaction imparted to it is sourced by the presence of a uniform distribution of heavy static quarks. The TFD state we consider here holographically corresponds to an entangled state of two AdS blackholes, each of which is deformed by a uniform distribution of static strings. In order to make a holographic estimation of correlation between two entangled boundary field theories in presence of backreaction we compute the holographic mutual information in the backreacted eternal blackhole. The late time exponential growth of an early perturbation is a signature of chaos in the boundary thermal field theory. Using the shock wave analysis in the dual bulk theory, we characterize this chaotic behaviour by computing the holographic butterfly velocity. We find that there is a reduction in the butterfly velocity due to a correction term that depends on the backreaction parameter. The late time exponential growth of an early perturbation destroys the two-sided correlation, whereas the backreaction always acts in favour of it. Finally we</p>

	compute the entanglement velocity that essentially encodes the rate of disruption of correlation between two boundary theories.
4.	<p>A novel diagnosis method for inter-turn short-circuits in srms by tracking post turn-off phase currents under current chopping control M Alam, N Gugulothu, S Payami - IEEE Transactions on Industrial Electronics, 2023</p> <p>Abstract: Current chopping control (CCC) is widely preferred for low and medium-speed applications in switched reluctance motor drives. With precise current regulation, the consequence of inter-turn short-circuits is not reflected much in the faulty phase current. Also, the fault features are difficult to extract in the online mode for minor short-circuits. Moreover, ITSCs are responsible for hot spots in the defective winding, ultimately leading to a complete winding short-circuit due to persisting heating effect. Even the associated complications of SRMs like torque ripple, noise and vibrations are amplified to a greater extent under ITSCs. Therefore, diagnosing ITSCs is critical to shun such unwanted characteristics and failures. This article proposes a simple and novel method to diagnose ITSCs even with minor short-circuits in SRMs operating under CCC. With the reduction in the inductance due to ITSCs, the decay time of the faulty phase current post turn-off also reduces. This variation is monitored for all the phase currents within their respective aligned rotor positions to diagnose ITSC. The proposed method has better detection reliability regarding diagnosis under varying load conditions. The scheme is validated experimentally on a test setup of a customized four-phase SRM having winding taps for emulating ITSCs.</p>
5.	<p>A residential-community-level load management scheme under semi-regulated distribution environment S Dash, R Sodhi, B Sodhi - Proceedings of the 11th International Conference on Innovative Smart Grid Technologies: IEEE PES Innovative Smart Grid Technologies, 2023</p> <p>Abstract: This paper proposes an electric load management model in a residential community to assist the utility in a semi-regulated distribution environment in handling the unforeseen surges in energy demand. The task is addressed by two layers of clustered priorities to fairly distribute the mismatch burden 1) across the appliances of each residence and 2) every residence of the community under each substation. The resulted multi-criteria decision problem is solved using integer programming on MATLAB with modified Pecan Street Database and IEEE-123 bus system. Test results reveal the efficacy of the proposed load management model in reducing energy consumption during the peak demand hours while providing a reliable power supply to the vital residential loads to reduce the comfort-loss.</p>
6.	<p>A small molecule potent IRAK4 inhibitor abrogates lipopolysaccharide-induced macrophage inflammation in-vitro and in-vivo SA Choudhary, D Patra, A Sinha, S Mazumder, R Pant...D Pal - European Journal of Pharmacology, 2023</p> <p>Abstract: Increasing evidence supports vanillin and its analogs as potent toll-like receptor signaling inhibitors that strongly attenuate inflammation, though, the underlying molecular mechanism remains elusive. Here, we report that vanillin inhibits lipopolysaccharide (LPS)-induced toll-like receptor 4 activation in macrophages by targeting the myeloid differentiation primary-response gene 88 (MyD88)-dependent pathway through direct interaction and suppression of interleukin-1 receptor-associated kinase 4 (IRAK4) activity. Moreover, incubation of vanillin in cells expressing constitutively active forms of different toll-like receptor 4 signaling molecules revealed that vanillin could only able to block the ligand-independent constitutively activated IRAK4/1 or its upstream molecules-associated NF-κB activation and NF-κB transactivation along with the expression of various proinflammatory cytokines. A significant inhibition of LPS-induced IRAK4/MyD88, IRAK4/IRAK1, and IRAK1/TRAF6 association was evinced in response to vanillin treatment. Furthermore, mutations at Tyr262 and Asp329 residues</p>

in IRAK4 or modifications of 3-OMe and 4-OH side groups in vanillin, significantly reduced IRAK4 activity and vanillin function, respectively. Mice pretreated with vanillin followed by LPS challenge markedly impaired LPS-induced IRAK4 activation and inflammation in peritoneal macrophages. Thus, the present study posits vanillin as a novel and potent IRAK4 inhibitor and thus providing an opportunity for its therapeutic application in managing various inflammatory diseases.

Graphical Abstract:



[Adsorption of hexavalent chromium by magnetite particles synthesized at various temperatures: effect of magnetic properties of the particles on individual adsorption mechanisms](#)
 S Ganguly, S Ganguly – EGU General Assembly, 2023

7.

Abstract: Chromium (VI) [Cr(VI)] is abundantly used for several industrial applications especially in stainless steel production and as an anti-corrosive agent in ceramics, textile industries and tanneries. Despite its versatile uses, Cr (VI) is a major environmental threat and is a known carcinogen. Therefore, proper precaution must be implemented while working with Cr (VI) or while disposing it after use. Due to improper handling and lack of proper care, Cr(VI) is still found in industrial wastewaters or landfill sites. The Cr(VI) in landfills can leach into the ground during rainfall and can risk the contamination of the groundwater causing a health catastrophe when consumed. This study focuses on effective Cr(VI) remediation by the process of adsorption. Magnetite particles synthesized by co-precipitation method at various temperatures (room temperature of 25°C, 60°C and 90°C) are used as an absorbent for achieving maximum removal efficiency of Cr(VI) from water. An initial concentration of 10mg/l at pH 7.2 and time of contact 10 minutes is taken as the starting parameters for Cr(VI) for the batch adsorption studies. The surface morphology, chemical composition and the magnetic properties of the magnetite particles are determined from FESEM (Field Emission Scanning Electron Microscope), EDS (Energy-Dispersive Spectroscopy) and VSM (Vibrating Sample magnetometer) characterization methods, respectively. The synthesis of the magnetite particles at various temperatures can affect both its physical (mainly pore size, shape, texture etc.) and magnetic properties and therefore can pose significant changes on the adsorption efficiency. The effect of the magnetite particle dose, pH of Cr(VI), time of contact between the magnetite particles and Cr(VI) and the effect of the change in the concentration of Cr(VI) are predicted in this study. A special focus is given on determining the variation in the magnetic properties of the magnetite particles due to different temperatures of synthesis. In case of any such noteworthy change in the magnetic properties, the alteration in the individual adsorption capacities of the iron-oxide particles are highlighted in this study. Langmuir and Freundlich isotherm models are used to predict the adsorption mechanisms.

8.

[An empirical investigation of the effects of poverty and urbanization on environmental degradation: the case of sub-Saharan Africa](#)
 B Rakshit, P Jain, R Sharma, S Bardhan - Environmental Science and Pollution Research, 2023

Abstract: This study empirically investigates the effects of poverty and urbanization on environmental degradation for a sample of 43 sub-Saharan African (SSA) economies from 1995

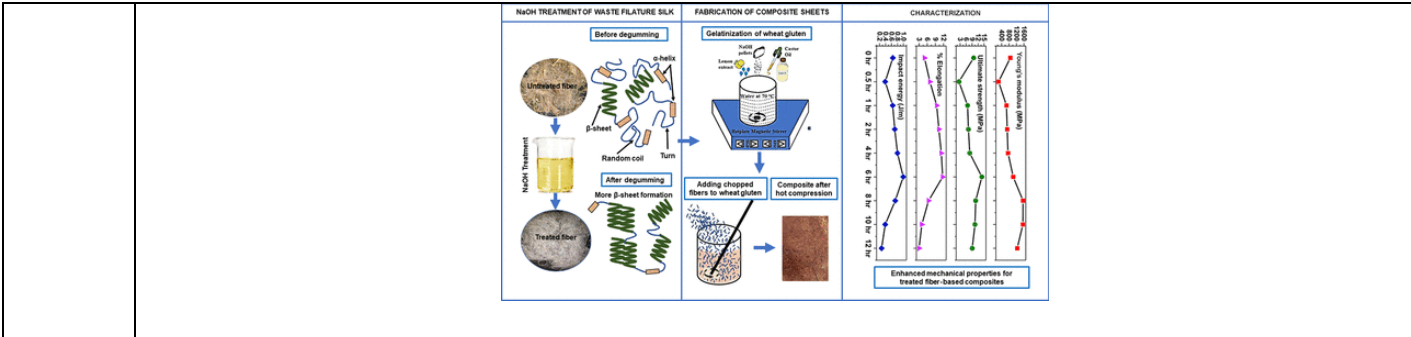
	<p>to 2018. The major contribution of the study lies in examining the existence of non-linear effects of poverty and urbanization on environmental degradation. We considered a set of institutional and demographic factors to explain the dynamics among poverty, urbanization, and environmental degradation. Findings suggest that an increase in the poverty gap significantly contributes towards intensifying environmental degradation in SSA countries. Results also show the existence of a non-linear relationship between poverty and environmental degradation. The findings purpose several crucial policy recommendations which necessitate the participation of different stakeholders such as government, institutions, researchers, non-profit organizations and citizens for the effective implementations of environment-friendly policies. A battery of robustness tests confirms the validity of the main findings of the study.</p>
9.	<p>Anti-cancer drug molecules targeting cancer cell cycle and proliferation D Patra, K Bhavya, P Ramprasad, M Kalia, D Pal - <i>Advances in Protein Chemistry and Structural Biology</i>, 2023</p> <p>Abstract: Cancer, a vicious clinical burden that potentiates maximum fatality for humankind, arises due to unregulated excessive cell division and proliferation through an eccentric expression of cell cycle regulator proteins. A set of evolutionarily conserved machinery controls the cell cycle in an extremely precise manner so that a cell that went through the cycle can produce a genetically identical copy. To achieve perfection, several checkpoints were placed in the cycle for surveillance; so, errors during the division were rectified by the repair strategies. However, irreparable damage leads to exit from the cell cycle and induces programmed cell death. In comparison to a normal cell, cancer cells facilitate the constitutive activation of many dormant proteins and impede negative regulators of the checkpoint. Extensive studies in the last few decades on cell division and proliferation of cancer cells elucidate the molecular mechanism of the cell-cycle regulators that are often targeted for the development of anti-cancer therapy. Each phase of the cell cycle has been regulated by a unique set of proteins including master regulators Cyclins, and CDKs, along with the accessory proteins such as CKI, Cdc25, error-responsive proteins, and various kinase proteins mainly WEE1 kinases, Polo-like kinases, and Aurora kinases that control cell division. Here in this chapter, we have analytically discussed the role of cell cycle regulators and proliferation factors in cancer progression and the rationale of using various cell cycle-targeting drug molecules as anti-cancer therapy.</p>
10.	<p>AV-GAZE: A study on the effectiveness of audio guided visual attention estimation for non-profilic faces S Ghosh, A Dhall, M Hayat, J Knibbe - <i>Proceedings of the IEEE International Conference on Image Processing</i>, 2022</p> <p>Abstract: In challenging real-life conditions such as extreme head-pose, occlusions, and low-resolution images where the visual information fails to estimate visual attention/gaze direction, audio signals could provide important and complementary information. In this paper, we explore if audio-guided coarse head-pose can further enhance visual attention estimation performance for non-prolific faces. Since it is difficult to annotate audio signals for estimating the head-pose of the speaker, we use off-the-shelf state-of-the-art models to facilitate cross-modal weak-supervision. During the training phase, the framework learns complementary information from synchronized audio-visual modality. Our model can utilize any of the available modalities i.e. audio, visual or audio-visual for task-specific inference. It is interesting to note that, when AV-Gaze is tested on benchmark datasets with these specific modalities, it achieves competitive results on multiple datasets, while being highly adaptive toward challenging scenarios.</p>
11.	<p>Comparison of single catheter versus dual catheter-based EBT3 film calibration for the Ir-192 beam energy G Trivedi, PP Singh, A Oinam - <i>Biomedical Physics & Engineering Express</i>, 2023</p> <p>Abstract: Purpose. Films and TLDs have been the common choices for passive in-vivo dose</p>

	<p>measurement in radiotherapy. In the brachytherapy applications, it is very difficult to report and verify the dose at multiple localized high dose gradient regions and also the dose to organ at risk. This study was carried out to introduce a new and accurate calibration method for GafChromic EBT3 films irradiated using Ir-192 photon energy from miniature High Dose Rate (HDR) Brachytherapy source. Materials and methods. Film holder made of Styrofoam was used to hold the EBT3 film at its center. It was placed inside the mini water phantom and the films were irradiated by Ir-192 source of microSelectron HDR afterloading brachytherapy system. Two different setups: Single catheter-based film exposure and dual catheter-based film exposure were compared. The films scanned on a flatbed scanner were analysed in three different color channels: red, green, and blue using Image J software. The dose calibration graphs were generated using the third-order polynomial equations fitted on the data points from two different methods of calibration procedure. Maximum and mean dose difference between TPS calculated and measured was analyzed. Results. The measured dose difference from the TPS calculated doses were evaluated for the three groups of dose ranges (low, medium and high). In the high dose range, standard uncertainty of dose difference are $\pm 2.3\%$, $\pm 2.9\%$, and $\pm 2.4\%$ respectively for the red, green, and blue color channel when the TPS calculated dose was compared with single catheter based film calibration equation. Whereas it is observed as 1.3%, 1.4% and 3.1% for the red, green, and blue color channels respectively when compared with the dual catheter based film calibration equation. A test film was exposed to a TPS calculated dose of 666 cGy to validate the calibration equations, single catheter based film calibration equation estimated the dose difference as -9.2%, -7.8% and -3.6% respectively in the red, green, and blue color channels whereas the same were observed as 0.1%, 0.2% and 6.1% respectively when dual catheter based film calibration equation was applied. Conclusion. Source miniature size, reproducible positioning of the film and catheter system inside water medium are the major challenges in the film calibration with Ir-192 beam. To overcome these situations dual catheter-based film calibration was found more accurate and reproducible as compare to the single catheter based film calibration.</p>
12.	<p>Computational aspects of double dominating sequences in graphs G Sharma, A Pandey - Conference on Algorithms and Discrete Applied Mathematics: Part of the Lecture Notes in Computer Science Book Series 2023</p> <p>Abstract: In a graph $G = (V, E)$, a vertex $u \in V$ dominates a vertex $v \in V$ if $v \in N_G[u]$. A sequence $S = (v_1, v_2, \dots, v_k)$ of vertices of G is called a double dominating sequence of G if (i) for each i, the vertex v_i dominates at least one vertex $u \in V$ which is dominated at most once by the previous vertices of S and, (ii) all vertices of G have been dominated at least twice by the vertices of S. GRUNDY DOUBLE DOMINATION problem asks to find a double dominating sequence of maximum length for a given graph G. In this paper, we prove that the decision version of the problem is NP-complete for bipartite and co-bipartite graphs. We look for the complexity status of the problem in the class of chain graphs which is a subclass of bipartite graphs. We use dynamic programming approach to solve this problem in chain graphs and propose an algorithm which outputs a Grundy double dominating sequence of a chain graph G in linear-time.</p>
13.	<p>Demonstrating deep learning driven bpsk demodulation using software-defined radios A Ahmad, S Agarwal - 15th International Conference on Communication Systems & Networks, 2023</p> <p>Abstract: Our objective in this demonstration is to demodulate the received BPSK signal using a deep neural network. In conventional demodulation, the performance is limited by the carrier frequency/phase offsets, hardware imperfections and use of multiple levels of nonlinear devices such as synchronizer, offset detector, etc. To improve the detection performance under high noise (i.e., low SNR), varying channel conditions and hardware impairments, we propose and demonstrate a deep neural network based demodulator which is able to detect bits even at lower SNRs. Results show that we can detect the received signal under synchronization offsets, varying</p>

	channel parameters and hardware imperfections due to its high proficiency in learning signal patterns and detecting the pattern embedded in noise. The demonstration will be carried out on USRP coupled with Matlab.
14.	<p>Design flood estimation based on equivalent geomorphological instantaneous unit hydrograph for a himalayan catchment S Rana, SR Chavan – EGU General Assembly, 2023</p> <p>Abstract: Recurrent flood estimation studies in Himalayan catchments located in India are crucial and require abundant monitoring and supervision. Reliable estimation of design floods for mountainous catchments corresponding to various return periods is challenging. Recently, climate change has exacerbated this challenge which pose a serious threat to the water resources within Himalayan region. The Geomorphology based Unit hydrograph theory can provide reliable estimates of design floods for Himalayan catchments. The theory involves determination of Geomorphological Instantaneous Unit Hydrograph (GIUH) corresponding to a catchment and utilizing the GIUH to predict design flood for a design rainfall input. In this study, it is envisaged to model the complex dynamics of floods in a Himalayan catchment by using a modified version of GIUH which is known as Equivalent Geomorphological Instantaneous Unit Hydrograph (E-GIUH). EGIUH overcomes many limitations associated with the conventional GIUH. The application of E-GIUH is performed for Seer catchment which is a sub-basin of Sutlej River basin. The design rainfall input to the E-GIUH is determined from Indian Meteorological Department (IMD) gridded rainfall data for the present (1951-2019) as well as the future time periods (2021-2060 and 2061-2100). Coupled Model Intercomparison Project phase 6 (CMIP6) experiments are considered to determine future projections of rainfall over Seer catchment which are subsequently used to estimate design rainfall input for future time periods. Design flood estimates are obtained for various Shared Socioeconomic Pathways (SSPs), particularly SSP126, SSP245 and SSP585 scenarios from CMIP6 experiments. The geomorphological descriptors used for development of E-GIUH model of the Seer catchment are evaluated using the GIS framework.</p>
15.	<p>Diagnosis of inter-turn short-circuits in srms by high frequency switching of phases amid low torque unaligned rotor positions M Alam, S Payami - IEEE Transactions on Industrial Electronics, 2023</p> <p>Abstract: The inherent problems of torque ripple, noise and vibrations associated with switched reluctance motors (SRMs) are escalated when the machine is subjected to inter-turn short-circuits (ITSCs). Also, leaving it unchecked can ultimately lead to a complete winding short-circuit due to the insulation failure owing to the heat produced by locally generated hotspots. To avoid such ruinous damage, the diagnosis of ITSCs is very critical. This article proposes a method of diagnosing ITSCs by injecting high-frequency signals in the phases in their low torque regions around unaligned rotor positions. The proposed method utilizes the drive power converter to inject and diagnose the ITSCs and thus requires no additional hardware. It has a higher sensitivity even toward minor fault conditions, i.e., as low as ITSC of 4 turns ($\approx 4\%$ ITSC over a phase). The devised fault indicator is immune to load or speed variation and, hence, better detection reliability. Also, the method can diagnose the fault under load and speed transients proving it to be more robust. Experiments are performed on a test rig of customized 8/6 SRM emulating the ITSCs to verify the potency of the proposed scheme.</p>
16.	<p>Digital disruption in the indian healthcare system S Roy - Practical Artificial Intelligence for Internet of Medical Things: A book chapter, 2023</p> <p>Abstract: The chapter begins with an introduction of the healthcare system in India, its challenges, and solutions to overcome the problems in the healthcare system. The second section of the chapter discusses the story and root cause of the coronavirus pandemic, which devastated the entire health ecosystem in India. Health crisis leads to an opportunity in the third section of</p>

	<p>the chapter; it throws light on the amalgamation of digital technology in the healthcare system, which brought a radical transformation. The rise in digital technologies in the healthcare domain increases efficiency, accessibility, and affordability. Integrating technologies like artificial intelligence, big data, and virtual reality solves institutional medical problems. The fourth section of the chapter discusses the health-tech start-up landscape in India and throws light on how the government bodies provide schemes and grants to encourage the start-up's ecosystem in the health domain. Finally, in the conclusion and recommendation sections, authors discussed the existing and future scope of digital healthcare sector in India.</p>
17.	<p>Do religious freedom vis-a-vis trade openness affect economic growth? a cross-country empirical investigation SR Behera, T Mishra, DP Dash - Theoretical Economics Letters, 2023</p> <p>Abstract: Does religious freedom steer economic growth impact of trade-openness? This paper employs the method of moments-quantile regression to panel data of 117 developed and developing countries to show that countries that accommodate greater liberal religious beliefs enjoy, on average, higher growth in per capita income via deeper trade openness. Empirical results reveal that the dynamic nexus between trade and economic growth across developing countries is subject to the institutional environment. Therefore, results indicate that trade openness favours economic growth when institutional quality improves.</p>
18.	<p>Does bank competition affect the transmission mechanism of monetary policy through bank lending channel? Evidence from India B Rakshit, S Bardhan - Journal of Asian Economics, 2023</p> <p>Abstract: This paper empirically investigates how intensified competition in the Indian banking affects the transmission of monetary policy through bank lending channel over the period 1997–2017. Additionally, this study examines the impact of deposit and loan market channels on bank's credit growth. Results obtained through two-step system-GMM reveal that a higher degree of market power weakens the monetary policy transmission mechanism for the entire banking industry and across ownerships. Results show that higher market power in the deposit and loan markets weakens the impact of monetary policy on bank loan supply. The findings of this study extend important policy measures that can strengthen the transmission mechanism of monetary policy by reducing the adverse effects of changes in bank competition.</p>
19.	<p>Dynamics of the panchi nala glacier, western himalaya: trends and controlling factors. M Prajapati, PK Garg, A Shukla, S Guha – EGU General Assembly, 2023</p> <p>Abstract: Information on glacier velocity is imperative to understand glacier mass, ice volume, topography, surge events of the glacier and response to climate change. Therefore, inter-annual surface ice velocity (SIV) of the Panchi Nala glacier has been calculated in the current study between the first two decades of the twenty-first century. To do so, the SIV has been computed by the feature tracking technique using the Co-registration of Optically Sensed Images and Correlation (COSI-Corr) method applied on the multi-temporal Landsat (TM and OLI) and sentinel -2 MSI images acquired between 2000 and 2021. The results of the study show that the mean velocity of the debris-covered tongue of the Panchi Nala Glacier is $\sim 10.60 \pm 5.56$ m/y during the study period. Additionally, the highest average glacier velocity is 13.77 ± 4.64 m/y, whereas the lowest is 8.92 ± 2.78 m/y, respectively, observed in 2005 and 2015. Also, the 95% confidence interval of the mean annual velocity lies between 9.76 and 11.43 m/y during the entire study period. The annual heterogeneity is linked with the variation of summer precipitation. Statistically, a 100 mm increment of summer precipitation can reduce the velocity around 1.3 m/y. The main reason behind this is the Panchi Nala glacier is located in high-elevation where the climate is much colder and during the summer precipitation, the lower temperatures cause the precipitation to take the form of snow, which freezes and accumulates on the glacier. This reduces the process of basal sliding. Further, detailed investigations with</p>

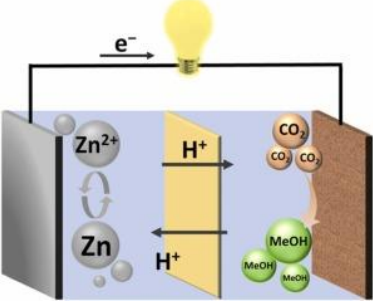
	<p>additional parameters need to be carried out to elucidate the comprehensive causes for inter-annual fluctuations in surface velocity. In this perspective, future research maybe directed towards higher temporal and spatial scale remote sensing-based investigations and validation of glacier surface velocity using field measurements, to better understand the glacier dynamics.</p>
20.	<p>Effect of cavity aspect ratio on mixed convective heat transfer phenomenon inside a lid-driven cavity due to elastic turbulence S Gupta, C Sasmal - <i>Physics of Fluids</i>, 2023</p> <p>Abstract: This study performs extensive numerical simulations to investigate how the aspect ratio of a lid-driven cavity influences the onset of elastic instability and elastic turbulence and the subsequent mixed convective heat transfer rate inside it. We find that the dependency of the cavity aspect ratio (AR) on the heat transfer rate is highly complicated depending upon the values of the Richardson (Ri) and Prandtl numbers (Pr). At low values of Ri, the heat transfer rate continuously decreases with AR irrespective of the value of the Prandtl number and the fluid type, i.e., Newtonian or viscoelastic. The same trend is also observed at high values of Ri and low values of Pr. At these combinations of Ri and Pr, the heat transfer rate is always higher in a viscoelastic fluid than in a Newtonian fluid due to the presence of elastic turbulence in the former fluid. However, a different trend is observed at high values of both Ri and Pr. At this combination of Ri and Pr, the heat transfer rate increases with AR in Newtonian fluids, whereas it decreases in viscoelastic fluids. Therefore, at high values of AR, Ri, and Pr, the heat transfer rate is found to be higher in Newtonian fluids compared to that in viscoelastic fluids despite the presence of elastic turbulence in the latter fluids. This is in contrast to the assumption that the elastic turbulence phenomenon always increases the rate of transport processes. A possible explanation for this behaviour is provided in this study.</p>
21.	<p>Effect of degumming duration on the behavior of waste filature silk-reinforced wheat gluten composite for sustainable applications P Bhowmik, R Kant, H Singh - <i>ACS Omega</i>, 2023</p> <p>Abstract: Silkworm silk proteins are of great importance in several fields of science owing to their outstanding properties. India generates waste silk fibers, also known as waste filature silk, in abundance. Utilizing waste filature silk as reinforcement in biopolymers enhances its physiochemical properties. However, the hydrophilic sericin layer on the surface of the fibers makes it very difficult to have proper fiber–matrix adhesion. Thus, degumming the fiber surface allows better control of the fiber properties. The present study uses filature silk (<i>Bombyx mori</i>) as fiber reinforcement to prepare wheat gluten-based natural composites for low-strength green applications. The fibers were degummed in sodium hydroxide (NaOH) solution from a 0 to 12 h duration, and composites were prepared from them. The analysis exhibited optimized fiber treatment duration and its effect on the composite properties. The traces of the sericin layer were found before 6 h of fiber treatment, which interrupted homogeneous fiber–matrix adhesion in the composite. The X-ray diffraction study showed enhanced crystallinity of the degummed fibers. The FTIR study of the prepared composites with degummed fibers showed that shifted peaks toward lower wavenumbers supported better bonding among the constituents. Similarly, the tensile and impact strength of the composite made of 6 h of degummed fibers showed better mechanical properties than others. The same can be validated with the SEM analysis and TGA as well. This study also showed that prolonged exposure to alkali solution reduces the fiber properties, thus reducing composite properties too. As a green alternative, the prepared composite sheets can potentially be applied in manufacturing seedling trays and one-time nursery pots.</p>



22. [Efficient CO₂ utilization and sustainable energy conversion via aqueous Zn-CO₂ batteries](#)
 S Kaur, M Kumar, D Gupta, PP Mohanty, T Das, S Chakraborty, R Ahuja, TC Nagaiah - Nano Energy, 2023

Abstract: Looking towards the economical and efficient carbon dioxide (CO₂) utilization, metal-CO₂ batteries uphold a great potential to enhance the efficiency of CO₂ conversion to fuels. Pertaining to this, we have fabricated B, N-containing carbon with tubular morphology (C-BN@600) derived from ionic liquid (IL) and metal-organic framework (MOF) composite as cathode catalyst with Zn foil anode for aqueous rechargeable Zn-CO₂ battery. The C-BN@600 catalyst demonstrate a remarkable activity towards electrochemical CO₂ reduction to methanol with a Faradaic efficiency of 74% and a Yield rate of 2665 μg h⁻¹ mg⁻¹ cat. The assembled battery consumes CO₂ continuously and electrochemically convert it to methanol during discharge and simultaneously produces electrical energy with a remarkable energy density of 330 Wh kg⁻¹ and a power density of 5.42 mW cm⁻² which is stable for more than 12 days (>300 h, 800 cycles) at 1 mA cm⁻², providing a platform to serve a dual purpose of CO₂ reduction and energy storage.

Graphical Abstract:

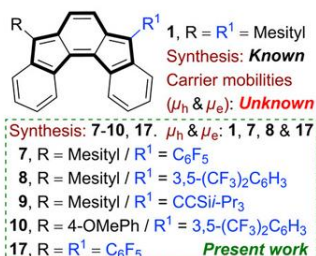


23. [Evaluation of damping effect influenced by system parameters on a dfig integrated power system](#)
 B Sahu, BP Padhy - IEEE Systems Journal, 2023

Abstract: Integration of doubly fed induction generator (DFIG)-based wind energy system (WES) introduces small-signal angular stability issues in synchronous generator dominated power systems. It is essential to understand the effect of system parameters on damping contribution by DFIG to the rest of the power system. This article presents a simplified mathematical formulation for analyzing system parameter's impact on the damping of interarea oscillations. A simple power system model consisting of two synchronous machines and a DFIG has been considered for mathematical derivations. For deriving the damping torque contribution to the rest of the power systems, DFIG has been used as a feedback system. The derived mathematical formulation has been validated for a higher order power system integrated with WES. The derived expression of damping contribution to synchronous machines supports the concept that the damping is highly dependent on transmission line reactance, which further assists the idea that WES placement in the power system has a crucial role in improving damping contribution to synchronous machines.

24.	<p>Experimental investigation of wc-12co cold sprayed: substrate hardness, bonding mechanism, powder type H Singh - Materials Today: Proceedings, 2023</p> <p>Abstract: Effects of substrate hardness and particle type on a single WC-12Co (Tungsten carbide cobalt) particle's deposition behavior during the cold spray process was investigated in this study. SEM was used to analyze the surface and cross-sections of the deposited particles to determine their morphology. It was discovered that the deposition behavior of WC-12Co particles changed with increasing substrate hardness, going from fully embedding into soft substrate to partially flattening and even rebounding from the hard substrate. Spherical microstructured WC-12Co particles sustained more severe deformation than other types of powder because of the smaller WC size. The porosity value of WC-12Co coatings is lower, at 1.18 %. WC-12Co particles bulk properties remained unchanged since there were no microstructural changes, decarburization, or the formation of fragile phases.</p>
25.	<p>Experimental investigation on the effect of in-cylinder heat release features on particle emissions characteristics of CNG–diesel RCCI engine MR Saxena, S Rana, RK Maurya - International Journal of Environmental Science and Technology, 2023</p> <p>Abstract: In-cylinder heat release features and nanoparticle emissions have been investigated in this study for CNG–diesel reactivity-controlled compression ignition (RCCI) engine. Study aims to determine the effect of low-temperature heat release (LTHR) and high-temperature heat release (HTHR) on the particles emissions from the RCCI engine. LTHR is obtained as a small peak (curve) before the main HTHR in the heat release rate curve. The LTHR and HTHR are not separated in heat release rate curve. The low-temperature heat release rate (LTHRR) is determined by extracting the heat release between start of combustion (SOC) to the intersection point of slope between LTHR and HTHR. The high-temperature heat release rate (HTHRR) is determined by fitting the trace between the intersection point of slope between LTHR and HTHR to the end of HTHR (the crank angle where the main HTHR turns negative after attaining the peak). This study calculates the amount of LTHR and HTHR by determining the absolute area under the LTHRR and HTHRR trajectories. Experiments are performed for different port-injected CNG masses (m_c) and engine loads at a fixed engine speed of 1500 rpm. Single- and double-fuel injection strategy is used for injecting diesel. In the double-injection strategy, two cases are investigated. In the first case, diesel mass is split in the ratio of 50:50% between the first and second injection, whereas in the second case, diesel mass is divided into the proportion of 70:30%. CNG fuel mass, diesel start of injection (SOI), and the number of injections are controlled by engine electronic control unit (ECU). Results indicates that at a lower load with single-injection strategy, the lower amount of LTHR promotes the formation of small particles for 30° bTDC diesel SOI. It is found that increase in m_c per cycle results in reduced and delayed LTHR and HTHR. With an increase in m_c, the amount of LTHR decreases, and the total PN increases. The reduction in LTHR with an increase in m_c leads to an increase in the formation of nucleation mode particles (NMPs) and a decrease in the accumulation mode particles (AMPs).</p>
26.	<p>Exploring indeno[2,1-c]fluorene antiaromatics with unsymmetrical disubstitution and balanced ambipolar charge-transport properties H Sharma, A Ankita, P Bhardwaj, UK Pandey, S Das – Organic Materials, 2023</p> <p>Abstract: Unsymmetrically disubstituted antiaromatic indenofluorene (IF), in comparison to aromatic pentacene counterpart with unsymmetrical disubstitution, was rare in the literature until our recent report on indeno[1,2-<i>b</i>]fluorene and indeno[2,1-<i>a</i>]fluorene. Described herein is a straightforward access to unsymmetrically disubstituted indeno[2,1-<i>c</i>]fluorenes bearing mesityl at one apical carbon and C₆F₅, 3,5-(CF₃)₂C₆H₃, and CCSi^{<i>i</i>}-Pr₃ at the other apical carbon, including 4-methoxyphenyl/3,5-(CF₃)₂C₆H₃ push/pull substitution at the apical carbons with</p>

appreciable orbital density, and a previously unknown symmetrically C₆F₅-disubstituted [2,1-*c*]IF. The electronic properties of the unsymmetrical derivatives lie halfway in between the two symmetrical counterparts, while the 4-methoxyphenyl derivative showed the smallest HOMO–LUMO energy gap and near-infrared absorption with intramolecular charge transfer character. Single-crystal analyses showed 1D-columnar stacks for the unsymmetrical motif with the C₆F₅ units co-facially π -stacked with the IF core, whereas symmetrically C₆F₅-disubstituted [2,1-*c*]IF, with a low-lying LUMO, showed intermolecular π – π stacks between the IFs that resulted in good electron mobility ($\mu_e = 8.66 \times 10^{-3} \text{ cm}^2 \cdot \text{V}^{-1} \cdot \text{s}^{-1}$) under space charge limited current measurements. Importantly, balanced ambipolar charge-transport behaviour could be extracted for an IF series with symmetrical/unsymmetrical substitutions, in comparison to its π -contracted pentalene congener.



[Functional connectivity signatures of major depressive disorder: machine learning analysis of two multicenter neuroimaging studies](#)

S Gallo, A El-Gazzar, P Zhutovsky, RM Thomas...D Bathula... - *Molecular Psychiatry*, 2023

27.

Abstract: The promise of machine learning has fueled the hope for developing diagnostic tools for psychiatry. Initial studies showed high accuracy for the identification of major depressive disorder (MDD) with resting-state connectivity, but progress has been hampered by the absence of large datasets. Here we used regular machine learning and advanced deep learning algorithms to differentiate patients with MDD from healthy controls and identify neurophysiological signatures of depression in two of the largest resting-state datasets for MDD. We obtained resting-state functional magnetic resonance imaging data from the REST-meta-MDD ($N = 2338$) and PsyMRI ($N = 1039$) consortia. Classification of functional connectivity matrices was done using support vector machines (SVM) and graph convolutional neural networks (GCN), and performance was evaluated using 5-fold cross-validation. Features were visualized using GCN-Explainer, an ablation study and univariate t-testing. The results showed a mean classification accuracy of 61% for MDD versus controls. Mean accuracy for classifying (non-)medicated subgroups was 62%. Sex classification accuracy was substantially better across datasets (73–81%). Visualization of the results showed that classifications were driven by stronger thalamic connections in both datasets, while nearly all other connections were weaker with small univariate effect sizes. These results suggest that whole brain resting-state connectivity is a reliable though poor biomarker for MDD, presumably due to disease heterogeneity as further supported by the higher accuracy for sex classification using the same methods. Deep learning revealed thalamic hyperconnectivity as a prominent neurophysiological signature of depression in both multicenter studies, which may guide the development of biomarkers in future studies.

28.

[Hydrogen-assisted intergranular fatigue crack initiation in metals: Role of grain boundaries and triple junctions](#)

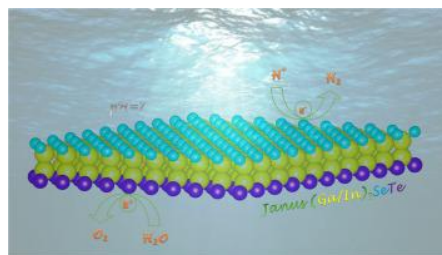
R Kumar, A Arora, DK Mahajan - *International Journal of Hydrogen Energy*, 2023

Abstract: In this work, small-scale, low-cycle fatigue experiments on hydrogen charged nickel specimens are performed that highlight particular grain boundaries (GBs) and triple junctions as potential intergranular crack initiation sites. To understand the micromechanics and underlying

	<p>physics, a dislocation density-based crystal plasticity model coupled with slip-rate based hydrogen transport model is developed. A fatigue indicator parameter (FIP) is also developed that models the crack initiation process by considering the contributions of accumulated plastic slip, GB normal stress, and local hydrogen concentration. Depending on the diffusivity, hydrogen binding energy, and misorientation, GBs are categorized as ‘special’ or ‘random’, and their role on hydrogen distribution is analysed using a model microstructure. Special GBs are ones with low diffusivity and high hydrogen binding energy whereas the random GBs have high diffusivity but low hydrogen binding energy. Complying with the experimental observations, the evolution of FIP with load cycles suggests certain triple junction configurations in the microstructure involving in the crack initiation process. For the case of uniform initial hydrogen concentration, special GBs are found to retain more hydrogen with load cycles primarily due to their low hydrogen diffusivity whereas the random GBs diffuse hydrogen out quickly to the bulk. The high hydrogen concentration and favourable stress state in the form of high hydrostatic stress spots generally found at triple junction of special/random GBs fulfil the necessary condition leading to an intergranular crack initiation.</p>
29.	<p>Hygrothermally stable stacking sequence for tailoring of extension–twist coupling in composite structures NK Shakya, SS Padhee - Composite Structures, 2023</p> <p>Abstract: Elastic coupling between in-plane and out-of-plane deformation modes is achievable only through asymmetric laminate composite. However, these asymmetric laminates are hygrothermally in-stable and lead to dimensional instability of the structure. In the current paper, previously derived necessary and sufficient conditions to eliminate these hygrothermal instabilities are briefly discussed and used to achieve hygrothermally stable laminate with extension–twist coupling. For this purpose, a generalized stacking sequence is proposed for laminate with $4l$ plies. These stacking sequences inherently satisfy all the hygrothermal stability conditions. Therefore, the optimization of the proposed stacking sequence becomes an unconstrained optimization problem and has been done analytically. For the verification purpose, constraint numerical optimization has also been performed. Hygrothermal stability conditions serve as the constraint of numerical optimization. The robustness of both analytically and numerically optimized results is verified using sensitivity analysis. For large l current approach is proved to be better than the numerical approach as this reduces the large set of calculations to just one with a minor difference in optimized value. Sensitivity study showed that proposed approach is equally sensitive errors in optimized stacking sequence.</p>
30.	<p>Image, insoluble: filming the cosmic in the colour out of space S Basu, D Ray - The Medial Afterlives of HP Lovecraft: A Book Chapter, 2023</p> <p>Abstract: Adapting horror has always been a trial. While filmmakers struggle with recreating the unfamiliar, there is always a slippery possibility of losing suspense as the categories of reality collapse, with the human body projected as the recipient of the violence of the uncanny. While it seems easier with violence and the visceral, the celluloid often needs to rethink its representation methods when the source of the uncanny become elusive. Hence, when films deal with “the weird and the eerie”¹ rather than the visceral, the familiar boundaries implode as the distinctions between reality and the beyond dissolve. Thus, filmic texts since the 1980s are often sites where the known constructs crumble, any master narrative with a fixed isolatable source of crisis dissolves, themes of concern change into mindless incoherence, images become more symbolic, and horror becomes an intrusion into the orderliness of expected horror rationales.</p>
31.	<p>Janus Ga₂SeTe and In₂SeTe nanosheets: excellent photocatalysts for hydrogen production under neutral pH I Bouziani, I Essaoudi, A Ainane, R Ahuja - International Journal of Hydrogen Energy, 2023</p>

Abstract: In the past few years, Janus nanosheets have attracted much interest according to their specific structure and considerable potential to address the energy and environmental issues. Herein, the electronic, optical and photocatalytic properties of two-dimensional Janus Ga₂SeTe and In₂SeTe have been studied using ab-initio computations based on the density functional theory. The obtained results show that these nanomaterials exhibit a semiconductor behavior with direct and moderate bandgaps using hybrid HSE06 functional. Subsequently, the understudied compounds present suitable optical conductivity, absorption, transmission and reflectivity for water splitting under the ultraviolet–visible light irradiation. Interestingly, the band edge positions of Janus Ga₂SeTe and In₂SeTe excellently straddle the redox potentials of water under neutral pH. Additionally, the free energy values for the formation of H₂ from H adsorbed on the Ga₂SeTe and In₂SeTe compounds are respectively 1.304eV and 0.976eV at pH = 7. More excitingly, the present study proposes strain engineering approach to improve the photocatalytic performance of the Janus Ga₂SeTe and In₂SeTe monolayers. Specifically, the investigated semiconductors show more appropriate band edge alignment and better hydrogen evolution reaction activity under biaxial tensile strain, which fulfil the water splitting requirements at neutral pH conditions. Our findings conclude that the Janus Ga₂SeTe and In₂SeTe nanosheets are promising candidates for photocatalytic hydrogen production.

Graphical Abstract:



[Linking changes in gangotri glacier features derived at a large-scale with climate variability](#)
 KV Mitkari, S Sofat, MK Arora, RK Tiwari – EGU General Assembly, 2023

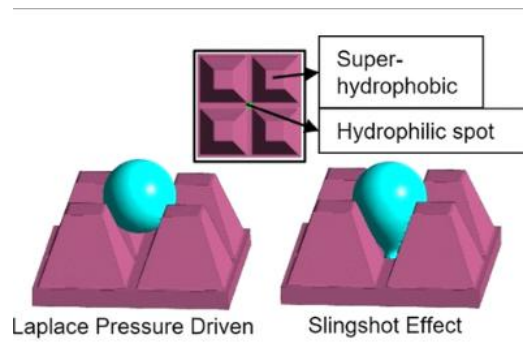
32.

Abstract: Changes in glacier area, snow, ice, debris cover, and other geomorphological features such as debris cones have a significant impact on the glacial dynamics, are a direct measure of glacier advance and retreat, form a critical input for measuring glacier mass balance, help identify the location of equilibrium line altitude, contribute to the global sea-level rise, and are a good index for understanding local climatic changes. Formation of glacial lakes enhance the rate of glacial melting and catastrophic events arising out of the outburst of glacial lakes can have serious impacts on the human life and economy. So, monitoring the spatial and temporal changes of glacier surface as well as non-surface features is imperative for assessing the health of glaciers and their behavior toward the climate change. The availability of high spatial resolution remote sensing images, has made precise mapping and monitoring of the changes in the glacier surface features and geomorphological features viable at a local level using object-based change detection (OBCD) rather than traditional pixel-based change detection (PBCD). OBCD has been used in numerous applications however, it has received little attention within the glaciological community. Advantage of using OBCD over PBCD is that the object-based paradigm enables the characterization of different land cover classes within the same image, using different object sizes. Further, in OBCD, each image object is considered as a single entity and hence, the small spurious changes and misregistration errors that occur due to high spectral variability are reduced because segmentation generates image objects which are less sensitive to the small spurious changes and misregistration respectively. Furthermore, a comprehensive literature survey on the Gangotri Glacier, Indian Himalayas uncovered that so far, no work has been done linking the variation of glacier surface and non-surface features with the important climate variables that is,

	<p>temperature and precipitation. Therefore, this study has evaluated the changes in the Gangotri Glacier features at a large scale using class OBCD approach from high spatial resolution WorldView-2 and LISS-4 images for a three-year period from 2011-2014. The meteorological data of Gangotri Glacier was obtained from Climate Research Unit Time Series v.4.06 dataset. A surge in the annual mean temperature and decline in the annual precipitation caused snow/ice area reduction by ~52%. This is accompanied by an increase in the ice-mixed debris (IMD) area by ~11%. The increase in IMD may lead to enhanced ice melting as it could reflect less incoming solar radiations. This further should have revealed expansion in supraglacial debris (SGD) area, however, it has minimized by ~0.4% which is justified with a rise in the periglacial debris (PGD) and debris cones by ~21% and ~9% respectively. Ascend in the annual mean temperature has also shown an increase of ~70% in the area of supraglacial lakes (SGLs), though the number of SGLs decreased; decrease in the number of SGLs suggests widening of SGLs in area. Thus, the dynamics of the glacier features is greatly affected by the yearly temperature and precipitation alterations in the area.</p>
33.	<p>Medical vqa: mixup helps keeping it simple J Singh, D Mahapatra, DR Bathula - International Conference on Image and Vision Computing: A Book Chapter, 2023</p> <p>Abstract: Recently, Medical Visual Question Answering (VQA) became an active area of research with the induction of several publicly available benchmark datasets and the organization of challenges. Like many competitions, the quest for success has driven the use of increasingly complex neural networks. Winning strategies generally leverage multi-scale architectures and model ensembling to achieve state-of-the-art performance. However, several studies have established the capability of simpler architectures in learning more meaningful features and avoiding over-parameterization. Specifically, the use of MixUp based image augmentation with a simple VGG16 network helped achieve significant improvement in performance for medical VQA. Inspired by this finding, we propose a modified version, VQAMixUp, that leverages both images and questions for augmenting VQA datasets. VQAMixUp combined with a few enhanced training strategies help simple models (with ~65% reduced parameters) achieve state-of-the-performance on benchmark ImageCLEF-VQA-MED validation datasets.</p>
34.	<p>Modelling of hydrogen-assisted damage at the deforming single crystal crack-tip R Kumar, DK Mahajan - Mechanics of Materials, 2023</p> <p>Abstract: A coupled framework of dislocation density-based crystal plasticity model and slip-rate based hydrogen transport model is developed to simulate hydrogen-assisted damage at the deforming crack-tip. Chemical potential-based boundary conditions and mobile dislocation-assisted hydrogen transport account for the evolving hydrogen concentration. A novel fracture indicator parameter is proposed to quantify the damage that considers the combined effect of local hydrogen concentration, accumulated plastic slip and stress triaxiality. Experimentally-informed critical value for hydrogen concentration is considered to model the crack initiation. Depending on the crystal orientation, the damage is shown to be associated either with an individual hydrogen embrittlement mechanism (hydrogen-enhanced localized plasticity, and hydrogen-enhanced decohesion) or their synergistic effect at the crack tip.</p>
35.	<p>Non-equilibrium processes in an unconserved network model with limited resources A Gupta, AK Gupta - The European Physical Journal Plus, 2023</p> <p>Abstract: We present a study of a peculiar form of network topology comprising of lanes connected via a junction, competing for particles in a reservoir of limited capacity with non-conserving dynamics. We exploit mean-field approximation to thoroughly analyze stationary dynamic properties such density profiles, phase boundaries, and phase diagrams. The steady-state properties have been studied by taking into account the time evolution of particle density. It is found that the ratio of the number of incoming and outgoing lanes from the network junction</p>

	<p>as well as that of the kinetic rates substantially influences the number of stationary phases and the complexity of the phase diagram concerning the increasing number of particles in the system. The maximal current phase can persist in a fragment or the complete lanes, when the number of incoming and outgoing lanes is equal, as opposed to unequal counterparts. For lower values of the total number of particles, only low density phase is achieved in the left subsystem. All the theoretical findings are supported by extensive Monte Carlo simulations and explained using simple physical arguments.</p>
36.	<p>Numerical and optimization-based study on split hemispherical shaped fins for augmenting heat transfer rate A Ranjan, R Das, SS Gajghate, D Barik, H Majumder... - International Journal of Energy Research, 2023</p> <p>Abstract: This paper deals with the numerical investigation of split hemispherical fins mounted staggered over a base plate. The thermal and flow analyses have been carried out to evaluate the Nusselt number (Nu), pressure drop, and hydrothermal performance factor (HTPF) with air as a medium and Reynolds number (to 15000). The cylindrical fin (CF) and hemispherical fin (HF, of radius) of the same volume and height have been formed and placed in the computational domain. Results reveal that the Nu for CF compared to HF is 1.3-1.4 times higher, with approximately 1.5 times higher for the given Re range. The value of HTPF for HF is greater than unity (/1.13-1.20) for all the considered Re values. Secondly, the HF gets split into longitudinal and transverse flow directions for better solid-fluid interaction. The geometrical parameters are transverse offset TO (/=), longitudinal offset LO (/=), and Re. Results show that the highest value of Nu (/=384.10) and HTPF (/=1.33) have been obtained at (at LO=0) and (at) for the highest Re (/=15000). At last, the cuckoo search algorithm (CSA) coupled with the response surface method (RSM) has been performed to fetch the optimum value of Nu based upon dimensionless TO, dimensionless LO, and Re. The optimum value (obtained at , , and) of Nu (=392.16) from CSA is promising, with the numerically obtained Nu value (=384.1059) with an error of 2.05%.</p>
37.	<p>Optimization of a salt gradient solar pond for air heating application S Verma, R Das - Journal of Physics: Conference Series, 2023</p> <p>Abstract: In this study, it is demonstrated that when a solar pond is used for an air heating application like crop drying, domestic space heating, greenhouse heating etc., it is important to account for pumping power in the calculations. When air is the working fluid, the magnitudes of extraction and pumping power are comparable. Therefore, a new parameter is defined in context of solar ponds used for air heating, namely, effective power (defined as power extracted minus pumping power). At first, using a steady-state analysis, a closed form solution is derived for extraction power. The pertinent expression for pumping power is taken from the literature. Thus, an analytical expression for effective power is obtained and thereafter, an optimization analysis has been carried with the objective of maximizing this effective power. The analysis is used to calculate optimum values of air mass flow rate and pond's non-convective zone thickness at which maximum effective power is registered. The corresponding maximum effective power and the associated air outlet temperature are also calculated. This work thus is believed to prove useful for designing of solar ponds that are used for air heating applications in a manner to ensure maximal system performance.</p>
38.	<p>Out-of-plane biphilic surface structuring for enhanced capillary-driven dropwise condensation L Stendardo, A Milionis, G Kokkoris, C Stamatopoulos, CS Sharma, R Kumar, M Donati, D Poulidakos - Langmuir, 2023</p> <p>Abstract: Rapid and sustained condensate droplet departure from a surface is key toward achieving high heat-transfer rates in condensation, a physical process critical to a broad range of industrial and societal applications. Despite the progress in enhancing condensation heat transfer</p>

through inducing its dropwise mode with hydrophobic materials, sophisticated surface engineering methods that can lead to further enhancement of heat transfer are still highly desirable. Here, by employing a three-dimensional, multiphase computational approach, we present an effective out-of-plane biphilic surface topography, which reveals an unexplored capillarity-driven departure mechanism of condensate droplets. This texture consists of biphilic diverging microcavities wherein a matrix of small hydrophilic spots is placed at their bottom, that is, among the pyramid-shaped, superhydrophobic microtextures forming the cavities. We show that an optimal combination of the hydrophilic spots and the angles of the pyramidal structures can achieve high deformational stretching of the droplets, eventually realizing an impressive “slingshot-like” droplet ejection process from the texture. Such a droplet departure mechanism has the potential to reduce the droplet ejection volume and thus enhance the overall condensation efficiency, compared to coalescence-initiated droplet jumping from other state-of-the-art surfaces. Simulations have shown that optimal pyramid-shaped biphilic microstructures can provoke droplet self-ejection at low volumes, up to 56% lower than superhydrophobic straight pillars, revealing a promising new surface microtexture design strategy toward enhancing the condensation heat-transfer efficiency and water harvesting capabilities.



[Performance analysis of a waste heat exchanger with thick separating wall working as a storage medium for continuous operation](#)

S Verma, C Aggarwal, R Das - *Journal of Energy Storage*, 2023

39.

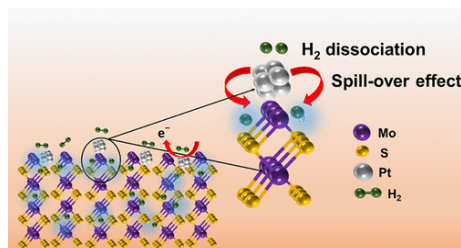
Abstract: In this study, a waste heat exchanger with a thick separating wall has been proposed to meet the off-waste heat period's energy requirement i.e., to store some of the waste heat energy when it is available and use it when waste heat is not available. Governing equations have been solved considering both lateral as well as longitudinal conduction in the separating wall through a two dimensional-transient model. The implicit finite difference method has been used to obtain the solution. The results reveals that a sufficiently thick wall separating the fluid streams in the waste heat exchanger can serve as a suitable heat storage medium and can behave as the heat source when the waste hot fluid is not available, thereby allowing a continuous operation. Further, the effects of various user-controlled parameters i.e., exchanger length, its width, fluid mass flow rates, thickness of the separating wall and thicknesses of the fluid flow passages on the system performance have been investigated. It is observed that increasing the exchanger length, its width, thicknesses of the separating wall and cold fluid flow passage reduce the outlet cold fluid temperature during the time waste heat is available, while the opposite effect is exhibited when waste heat is unavailable. Increasing the hot and cold fluid mass flow rates increases and decreases the extraction temperature at all times respectively. Finally, enhanced hot fluid flow passage thickness causes reduced output at all times. The reasons behind these parametric influences are discussed in detail. This work can therefore serve as a guiding study for designing such a heat exchanger with thermal storage capability.

40.

[Performance assessment of solar and desiccant aided building air-conditioning system](#)
G Singh, R Das - *Journal of Physics: Conference Series*, 2023

	<p>Abstract: Indoor thermal comfort significantly influences people's health, happiness and consequently the output at the workplace. Here, a systematic simulation study on a conventional vapor compression-based building cooling system integrated with desiccant assisted dedicated outdoor air system (DOAS) is performed using EnergyPlus software for warm and humid climate zones. Impact of using desiccant material in the DOAS, on the cooling load requirement of the building, coefficient of performance (COP), and energy consumption of the system is discussed. The building design is well-validated with the available guidelines. Desiccant assisted system supplies dehumidified air inside the building space which affects the evaporator performance. A flat plate solar collector system is used to supply the hot air to regenerate the desiccant material. Electric energy savings in desiccant assisted system can be achieved up to 5.5 %, whereas, the COP of the system is not found to be significantly affected even though thermal load demand reduces by nearly 13.5 % by the proposed modification.</p>
41.	<p><u>Phenomenology and kinetics of sessile droplet evaporation on convex contours</u> A Paul, RK Dash, P Dhar - <i>International Journal of Thermal Sciences</i>, 2023</p> <p>Abstract: In this article we probe experimentally and theoretically the evaporation phenomenology and kinetics of sessile droplets seated over convex hydrophilic and superhydrophobic (SH) surfaces. To understand the role of convex contours, both cylinders (mono-curvature system) and spheres (two-curvature system) have been explored. The evolution of the droplet shape during evaporation was monitored by optical imaging. The observations reveal improved evaporation rates on convex substrates, and the same tends to increase with increasing curvature. The findings also show that the influence of a two-curvature system (sphere) on the evaporation rate is to a higher extent than that for a mono-curvature system (cylinder). These observations are attributed to the augmented liquid-vapor interfacial area and widened up vapor diffusion domain which renders the liquid-molecules more scope to diffuse in the surrounding environment. The dynamic behavior of the triple line (TL) on convex substrates shows higher receding velocity of the contact line especially on spherical substrates. To visualize the internal flow and understand the effect of substrate convexity on internal advection dynamics, particle image velocimetry (PIV) was carried out. These results show higher strength of circulation velocity inside a droplet evaporating over convex surfaces despite frequent de-pinning of contact line. This behavior can be explicated by the fact than on convex surfaces higher temperature gradient exists along the liquid-vapor interface of the droplet (due to more evaporative cooling, and mapped through infrared thermography), which induces stronger thermal-Marangoni convection, thereby scaling up the circulation velocity. The finding may hold implications towards the design and development of droplet-based thermofluidic devices.</p>
42.	<p><u>Pt nanoparticles on vertically aligned large-area mos₂ flakes for selective h₂ sensing at room temperature</u> R Wadhwa, A Kumar, R Sarkar, PP Mohanty, D Kumar...R Ahuja...M Kumar - <i>ACS Applied Nano Materials</i>, 2023</p> <p>Abstract: The increasing demand of hydrogen (H₂) as an alternative clean fuel emboldened the parallel development of extremely sensitive room-temperature H₂ sensors for safety purposes. Molybdenum disulfide (MoS₂) is an intriguing material, exhibiting a high chemical sensing ability. However, usage of MoS₂ in H₂ sensors has been limited and usually suffers from low sensitivity and selectivity, especially at room temperature. In this work, we report a highly sensitive and selective H₂ sensor based on Pt nanoparticle-functionalized vertically aligned large-area MoS₂ flakes. The fabricated Pt@MoS₂ sensor exhibits a high sensitivity value of 23%, excellent reproducibility, fast response, and complete recovery at room temperature. The superior response of the sensor is attributed to the spillover effect and adsorption sites distributed on the Pt surface and the MoS₂-Pt interface. The influence of operating temperature on the sensing performance is also investigated. Density functional theory calculations validate our</p>

experimental results and demonstrate higher adsorption of H₂ for Pt@MoS₂ leading to improved and selective H₂ response. This study offers Pt nanoparticle-sensitized MoS₂ as a potential candidate for the development of low-power and room-temperature H₂ sensors for near future hydrogen vehicles and related technologies.



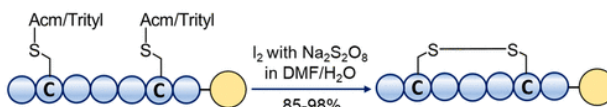
43. [Pv-aware replacement policy for two-level shared cache](#)
 B Agarwalla, N Sahu, S Das - IEEE International Symposium on Smart Electronic Systems, 2022

Abstract: The performance of modern multicore processes largely depends on the performance of their shared Last Level Cache (LLC). A larger LLC can reduce misses while increasing access latency. Tile-based chipmultiprocessors (TCMP) are also proposed with two levels of shared caches to handle such situations. Among the two levels of shared caches, the bottom level is designed with DRAM technology for better capacity, and the upper level is designed with SRAM technology for better latency. Because it is in the last level, the LLC is the DRAM-based shared cache. Both the shared caches are normally divided into multiple banks. The core in such TCMPs can have its own private cache above these two levels of shared caches. Process variation has been observed to have a much greater impact on DRAM-based memory chips than on SRAM-based memories. Hence, the banks of the DRAM-based LLC may not behave uniformly. Some of the banks may experience high energy costs and access latency because of PV. In this work, we have proposed a replacement policy for the SRAM-based shared cache (upper-level shared cache), which reduces the requirements to access the PV-affected LLC banks significantly. This is achieved by relaxing the blocks of the affected LLC banks to remain in the upper-level shared cache (SRAM-based) for a longer time. The experimental analysis found that the proposed replacement policy improves performance by 13%, 10%, and 6% as compared to three existing replacement policies.

44. [Rapid and highly productive assembly of a disulfide bond in solid-phase peptide macrocyclization](#)

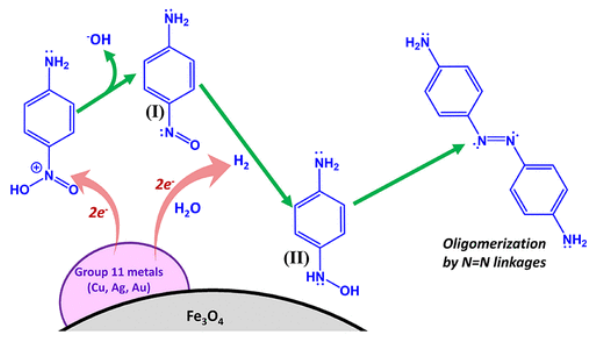
A Chowdhury, V Gour, BK Das, S Chatterjee, A Bandyopadhyay - Organic Letters, 2023

Abstract: Here we report a highly efficient disulfide-driven peptide macrocyclization in 15 min on a solid support using persulfate as a crucial additive in iodine-mediated oxidative cyclization. The method eliminates the side products of classical iodine-mediated peptide cyclization. It is operationally simple and convenient for cyclizing small to lengthier peptides embodying popular cysteine building blocks in a single step.



Example (FDA approved drugs): Vasopressin, Somatostatin, Terlipressin, iRGD, Lanreotide, Setmelanotide, and Tigerin-1

- ✓ The easily accessible Cys building blocks and oxidizing agents
- ✓ Operationally simple one-step process
- ✓ Time required 15 min
- ✓ Highly-efficient green and clean synthetic method

45.	<p>Real-time data acquisition and discharge pulse analysis in controlled RC circuit based Micro-EDM S Raza, R Nadda, CK Nirala - <i>Microsystem Technologies</i>, 2023</p> <p>Abstract: Owing to the non-isoenergetic discharge pulses in an RC-based micro-electrical discharge machining (μEDM) process, the unit material removal analysis is difficult. It requires a robust discharge pulse acquisition and monitoring system to capture, process and record live discharge data. Effective acquisition and monitoring of discharge pulses need an experimental diagnosis in real-time. The present work proposes a technology to monitor the discharge pulses of a controlled RC-based μEDM in real-time. Signals, while being acquired through various sensors, are processed in NI LABVIEW-based data acquisition (DAQ) system. Extensive virtual instrumentation is performed to categorize the discharge pulses in contributing, semi-contributing and non-contributing towards material removal, through an in-house developed pulse discrimination system (PDS). The developed PDS is simultaneously used to estimate the real-time discharge energies of individual pulses and their histograms with the machining progress. The acquired information from the developed PDS is used to justify the variations in discharge energy, material removal, and tool wear, with increasing machining depth. The PDS has shown the potential of predicting the conventionally unpredictable real-time unit volume removal during the process, which may be considered an important tool to meet the current industrial demands for remote access and monitoring of the process.</p>
46.	<p>Reductive oligomerization of nitroaniline catalyzed by Fe₃O₄ spheres decorated with group 11 metal nanoparticles CA Huerta-Aguilar, R Srivastava, JA Arenas-Alatorre... - <i>ACS Omega</i>, 2023</p> <p>Abstract: The present work demonstrates a simple and sustainable method for forming azo oligomers from low-value compounds such as nitroaniline. The reductive oligomerization of 4-nitroaniline was achieved via azo bonding using nanometric Fe₃O₄ spheres doped with metallic nanoparticles (Cu NPs, Ag NPs, and Au NPs), which were characterized by different analytical methods. The magnetic saturation (M_s) of the samples showed that they are magnetically recoverable from aqueous environments. The effective reduction of nitroaniline followed pseudo-first-order kinetics, reaching a maximum conversion of about 97%. Fe₃O₄-Au is the best catalyst, its a reaction rate ($k_{\text{Fe}_3\text{O}_4\text{-Au}} = 0.416 \text{ mM L}^{-1} \text{ min}^{-1}$) is about 20 times higher than that of bare Fe₃O₄ ($k_{\text{Fe}_3\text{O}_4} = 0.018 \text{ mM L}^{-1} \text{ min}^{-1}$). The formation of the two main products was determined by high-performance liquid chromatography-mass spectrometry (HPLC-MS), evidencing the effective oligomerization of NA through N = N azo linkage. It is consistent with the total carbon balance and the structural analysis by density functional theory (DFT)-based total energy. The first product, a six-unit azo oligomer, was formed at the beginning of the reaction through a shorter, two-unit molecule. The nitroaniline reduction is controllable and thermodynamically viable, as shown in the computational studies.</p>  <p style="text-align: right;"><i>Oligomerization by N=N linkages</i></p>
47.	<p>Rising temperature drives tipping points in mutualistic networks S Bhandary, S Deb, PS Dutta - <i>Royal Society Open Science</i>, 2023</p>

Abstract: The effect of climate warming on species' physiological parameters, including growth rate, mortality rate and handling time, is well established from empirical data. However, with an alarming rise in global temperature more than ever, predicting the interactive influence of these changes on mutualistic communities remains uncertain. Using 139 real plant–pollinator networks sampled across the globe and a modelling approach, we study the impact of species' individual thermal responses on mutualistic communities. We show that at low mutualistic strength plant–pollinator networks are at potential risk of rapid transitions at higher temperatures. Evidently, generalist species play a critical role in guiding tipping points in mutualistic networks. Further, we derive stability criteria for the networks in a range of temperatures using a two-dimensional reduced model. We identify network structures that can ascertain the delay of a community collapse. Until the end of this century, on account of increasing climate warming many real mutualistic networks are likely to be under the threat of sudden collapse, and we frame strategies to mitigate this. Together, our results indicate that knowing individual species' thermal responses and network structure can improve predictions for communities facing rapid transitions.

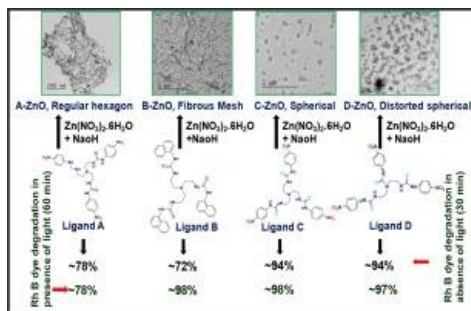
[Role of linker molecules on morphology of tripodal ligands based functionalized ZnO nanoparticles and its effect on photocatalysis](#)

J Mishra, G Singh, N Kaur, AK Ganguli - *Inorganic Chemistry Communications*, 2023

48.

Abstract: Photocatalysis using semiconductor nanoparticles is very popular method to degrade toxic dyes used in several industrial processes. ZnO is widely accepted material for application in photocatalysis because of its wide band gap (3–3.7 eV), biocompatibility and cost effectiveness. The properties of a photocatalyst can be tuned to desirable band gap, adsorption and catalytic sites by decreasing its size and modifying its surface. In this manuscript, ZnO nanomaterials with modified surface are prepared by using surface directing groups like urea/thiourea based tripodal ligands which help in obtaining particles with variable size as well as the surface characteristics. More importantly, synthesis of these ZnO nanoparticles is carried out at room temperature i.e. 30–40 °C. Four tripodal ligands **A** i.e. 1,1',1''-(2,2',2''-nitriлотris (ethane-2,1-diyl))tris(3-(4-nitrophenyl)urea), **B** i.e. 1,1',1''-(2,2',2''-nitriлотris(ethane-2,1-diyl))tris(3-(naphthalen-1-yl)urea), **C** i.e. [1,1',1''-(2,2',2''-nitriлотris (ethane-2,1-diyl))tris(3-(4-nitrophenyl)thiourea)] and **D** i.e. [1,1',1''-(2,2',2''-nitriлоbis(ethane-2,1-diyl))tris(3-(4-nitrophenyl)thiourea)]. These ligands are further used as structure directing agents for the synthesis of surface modified ZnO nanomaterials i.e. A-ZnO (regular hexagon), B-ZnO (fibrous mesh), C-ZnO (spherical) and d-ZnO (distorted spherical). Their photocatalytic study towards degradation of Rhodamine B dye revealed the efficiency of A-ZnO as 78 % while others as ~ 97–98 % in 60 min. Among them, C-ZnO and d-ZnO degraded ~ 94 % dye molecules within 30 min in absence of light (dark).

Graphical Abstract: Morphology control of surface modified ZnO nanoparticles by ligands A, B, C and D at room temperature and their catalytic activity towards Rh B dye degradation.



49.

[Salivary protein kinase C alpha and novel microRNAs as diagnostic and therapeutic resistance](#)

[markers for oral squamous cell carcinoma in Indian cohorts](#)

S Saproo, SS Sarkar, V Gautam, CW Konyak, G Dass, A Karmakar, M Sharma...S Naidu - Frontiers in Molecular Biosciences, 2023

Abstract: Oral squamous cell carcinoma (OSCC) is the second leading cause of cancer-related morbidity and mortality in India. Tobacco, alcohol, poor oral hygiene, and socio-economic factors remain causative for this high prevalence. Identification of non-invasive diagnostic markers tailored for Indian population can facilitate mass screening to reduce overall disease burden. Saliva offers non-invasive sampling and hosts a plethora of markers for OSCC diagnosis. Here, to capture the OSCC-specific salivary RNA markers suitable for Indian population, we performed RNA-sequencing of saliva from OSCC patients ($n = 9$) and normal controls ($n = 5$). Differential gene expression analysis detected an array of salivary RNAs including mRNAs, long non-coding RNAs, transfer-RNAs, and microRNAs specific to OSCC. Computational analysis and functional predictions identified protein kinase c alpha (PRKCA), miR-6087, miR-449b-5p, miR-3656, miR-326, miR-146b-5p, and miR-497-5p as potential salivary indicators of OSCC. Notably, higher expression of PRKCA, miR-6087 and miR-449b-5p were found to be associated with therapeutic resistance and poor survival, indicating their prognostic potential. In addition, sequencing reads that did not map to the human genome, showed alignments with microbial reference genomes. Metagenomic and statistical analysis of these microbial reads revealed a remarkable microbial dysbiosis between OSCC patients and normal controls. Moreover, the differentially abundant microbial taxa showed a significant association with tumor promoting pathways including inflammation and oxidative stress. Summarily, we provide an integrated landscape of OSCC-specific salivary RNAs relevant to Indian population which can be instrumental in devising non-invasive diagnostics for OSCC.

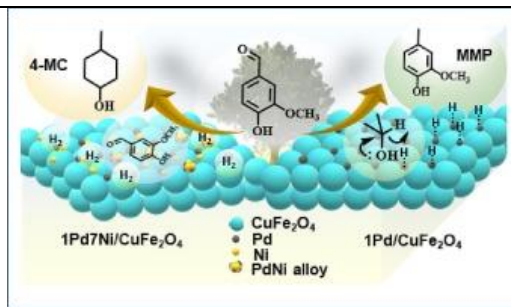
[Selective catalytic hydrodeoxygenation of vanillin to 2-Methoxy-4-methyl phenol and 4-Methyl cyclohexanol over Pd/CuFe₂O₄ and PdNi/CuFe₂O₄ catalysts](#)

GS More, DR Kanchan, A Banerjee, R Srivastava - Chemical Engineering Journal, 2023

50.

Abstract: The development of a sustainable catalytic process for the hydrodeoxygenation of lignin model compounds to renewable fuels and chemicals is essential to meet the requirement of a fossil-fuel-free modern society. Herein a Pd/CuFe₂O₄ and bimetallic PdNi/CuFe₂O₄ catalysts were developed for the hydrodeoxygenation of vanillin to 2-methoxy-4-methylphenol (MMP) and 4-methyl cyclohexanol (4-MC), respectively. The Pd/CuFe₂O₄ provided selective catalytic transfer hydrodeoxygenation of vanillin to MMP with isopropanol (IPA). The synergistic participation of Pd NPs and CuFe₂O₄ (1Pd/CuFe₂O₄) afforded 99.4% vanillin conversion and 99.2% MMP selectivity at 150 °C. The acidity of the catalyst facilitated the efficient adsorption of vanillin and IPA, and the high dispersion of Pd NPs lowered the hydrogen abstraction barrier of IPA to facilitate the transformation. Then Ni was incorporated into Pd/CuFe₂O₄ to produce 4-methyl cyclohexanol from vanillin. The interfacial interaction between Pd and Ni over CuFe₂O₄ (1Pd7Ni/CuFe₂O₄) provided 95.8% 4-methyl cyclohexanol (4-MC) in H₂ (20 bar) at 180 °C. The acidity of the catalyst, formation of Pd-Ni alloys, and efficient adsorption of vanillin and MMP were responsible for the high activity of the catalyst towards 4-methyl cyclohexanol (4-MC) production. Density functional theory (DFT) calculations were also performed to elucidate the reaction mechanism for vanillin transformation to MMP and 4-MC on the Pd/CuFe₂O₄ and bimetallic PdNi/CuFe₂O₄ catalysts.

Graphical Abstract:



[Strong entanglement criteria for mixed states, based on uncertainty relations](#)
 Manju, A Biswas, S Dasgupta - *Journal of Physics A: Mathematical and Theoretical*, 2023

51.

Abstract: We propose an entanglement criterion, specially designed for mixed states, based on uncertainty relation and the Wigner–Yanase skew information. The variances in this uncertainty relation do not involve any classical mixing uncertainty, and is therefore purely of quantum mechanical nature. We show that a large class of mixed entangled states can be characterized by our criterion. We demonstrate its utility for several generalized mixed entangled state including two-qubit and two-qutrit Werner states and it turns out, for the states discussed in this paper, to be stronger than any other known criterion in identifying the correct domain of relevant parameters for entanglement. The relevant uncertainty relation reduces to the Schrodinger–Robertson inequality for pure states.

[Superconducting state of the van der Waals layered PdH₂ structure at high pressure](#)
 P Tsuppayakorn-ae, A Majumdar, R Ahuja, T Bovornratanaraks, W Luo - *International Journal of Hydrogen Energy*, 2023

52.

Abstract: We report structural and superconducting transitions in layered van der Waals (vdW) palladium dihydride (PdH₂) calculated under high-pressure compression. PdH₂ has a Hexagonal Closed-Packed (HCP) structure with a space group of $P6_3mc$, and has a superconducting transition temperature of 24 K at ambient pressure. At 15 GPa, the crystalline to vdW layered structural transition occurs, while the superconductivity remains. On compressing from 15 to 50 GPa, the T_c increased abnormally by 3.5 K. It is found that the superconducting critical temperature of $P6_3mc$ PdH₂ is determined by the out-of-plane interlayer breathing vibrational mode. As a vdW layered metal hydride superconductor, PdH₂ provides a platform to study hydride superconductivity in such kinds of materials.

[Unified transformer network for multi-weather image restoration](#)
 A Kulkarni, SS Phutke, S Murala - *European Conference on Computer Vision: Part of the Lecture Notes in Computer Science Book Series*, 2023

53.

Abstract: Vision based applications routinely involve restoration as a preprocessing step, making it impossible to have separate architectures for different types of weather restoration. But, most of the existing methods focus on weather specific application. Further, the methods for multi-weather image restoration have high computational constraints. To overcome these limitations, we propose a compact transformer based network, with 4.5M parameters (1/10th of the existing method) for unified (simultaneous) removal of rain, snow and hazy effect with *single set of trained parameters*. We propose two parallel streams to handle the degradations: First, original resolution transformer stream (ORTS) focuses mainly on extracting fine level features through original scales of the inputs. Second, multi-level feature aggregation stream (MFAS) learns different sizes of the weather degradations. Further, it also uses coarse outputs from the first stream and utilizes edge boosting skip connections (EBSC) for propagating crucial edge details essential for image restoration. Finally, we present a memory replay training approach for

	generalization of the proposed network on multi-weather degraded scenarios. Substantial experiments on synthetic as well as real-world images, along with extensive ablation studies, demonstrate that the proposed method performs competitively with the existing methods for multi-weather image restoration. The code is provided at https://github.com/AshutoshKulkarni4998/UMWTransformer .
--	--

Disclaimer: This publication digest may not contain all the papers published. Library has compiled the publication data as per the alerts received from Scopus and Google Scholar for the affiliation “Indian Institute of Technology Ropar” for the month of February 2023. The author(s) are requested to share their missing paper(s) details if any, for the inclusion in the next publication digest.